

HULL GIRDER VIBRATION EFFECTS IN BENDING STRESSES MEASURED UNDER HARSH, STATIONARY CONDITIONS

Jan Mathisen, DNV, Norway
Robert Kjelstadli, DNV, Norway
Erlend Moe, DNV, Norway
Gaute Storhaug, DNV, Norway

SUMMARY

Wave-induced, hull girder vibration is known to have a significant effect on fatigue in some types of ships. Extensive measurements on ore and bulk carriers in service have been used to investigate and quantify these effects. A pilot study has been carried out in an attempt to use some of the same data to determine if there is also a significant effect on extreme wave loads. A few time series of hull bending stresses from two bulk carriers, operating in the North Atlantic iron ore trade, have been analysed. Harsh conditions due to a combination of waves, heading, speed and draught have been sought in order to approach extreme conditions. Somewhat milder conditions have also been included to investigate trends. Long, continuous records, which imply greater confidence in response statistics than is available from shorter records, have been obtained from harsh, stationary conditions. Low pass filtering has been applied to separate the ordinary, non-vibratory, wave-induced stresses from the total wave-induced stresses. Stress maxima and minima have been extracted from the time series and distribution functions have been fitted to these data. The results show a significant contribution to the total stress from the vibratory component, even under the harshest conditions that were available. This indicates that hull girder vibrations may need to be taken into account in the prediction of the extreme stresses in certain ship types.

1. INTRODUCTION

Det Norske Veritas is engaged in long term measurement programmes of hull stresses in a number of ships. The main objective of these programmes is related to the understanding and control of fatigue damage due to wave-induced, hull girder vibrations. Descriptions of some of these measurements and their results are given in [1] and [2]. The former paper also includes a survey of related research from many sources. The present paper attempts to use some of these measurements for a different purpose; viz. to investigate the effect of hull girder vibration under harsh conditions. This is intended to be one step along the path to extreme conditions. However, ship response under extreme conditions is rarely measured, if ever, such that extrapolation from measured response or prediction from calculated response is required. We are not prepared to attempt such extrapolation from the data that is available at present.

For ocean-going merchant ships, hull girder design against extreme loads tends to be based on quasi-static analysis, implying that the effects of hull girder vibrations are relatively small or negligible in the ultimate limit state, whereas these effects can be significant in the fatigue limit state. It is convenient to assume linear response to waves in the initial discussion of the differences between ship responses in these two limit states. It then follows that each frequency component in the hull response corresponds to the same frequency component of the wave spectrum. The longest natural period of hull vibration is typically around 2s (for a 300m long ship). Considerably longer wave periods, say above 10s, tend to induce the largest hull bending moments, because such waves are higher, and because they provide wavelengths in the vicinity of the ship

length, which generate bending moments more effectively. In reality, a sea state consists of a wide range of wave periods, but the amount of energy in the high frequency tail of the wave spectrum, in the vicinity of the lowest hull natural frequency, tends to be very small when the peak period is above 10s. This is the primary reason why dynamic analysis of the hull can be replaced with quasi-static analysis. Ship forward speed also affects this discussion. It induces a Doppler effect, such that head waves with a period of 4.3s provide an encounter period of 2s when the speed is 15 knots. Thus, forward speed in head waves tends to increase the amount of wave energy available to excite hull vibration. This is important for fatigue, which accumulates under a wide range of wave conditions. However, merchant ships are expected to have very little forward speed in the ultimate limit state, such that the Doppler effect is not so relevant there. Speed is reduced significantly due to added resistance in head waves from the blunt bows of tankers and bulk carriers, and voluntary speed reduction is also applied to avoid damage to the ship and discomfort. This is not necessarily the case for naval ships, which may have a greater need to make speed in severe waves.

If design changes are introduced that tend to lengthen the natural periods of hull vibration, then the effects of hull vibration will tend to become more important; e.g. the relatively long and flexible ships trading on the Great Lakes are more susceptible to hull vibration.

Linear analysis is a good method for predicting many aspects of ship response to waves, but it can be inadequate when resonance phenomena occur outside the frequency range of the encountered wave energy. One notable case concerns the low frequency oscillations of moored ships and offshore platforms, with natural

periods in the order of minutes, for which a nonlinear, second order theory is required. This provides excitation forces at other frequencies than the frequencies of the incoming waves. Excitation at difference frequencies, differences between the frequencies of all pairs of wave components in the wave spectrum, excites the resonant, low frequency response of moored systems. Second order theory also provides high frequency excitation at sum frequencies. This type of high frequency excitation is irrelevant for the moored systems, but contributes to hull girder vibrations [3].

Bottom and bow flare impacts are known to induce transient hull girder vibrations, usually referred to as whipping. This type of transient excitation force is not directly amenable to first or second order theory, although linear theory can be used to predict when wave impacts occur. On the other hand, stationary hull girder vibrations in the vertical plane are commonly referred to as springing. It can be difficult to distinguish between springing and whipping. The effects of gradual changes in hull form, in the bow or stern regions, away from the wall-sided assumption of linear theory, might be amenable to a second or higher order analysis. If so, this would be likely to provide a source of excitation for springing, with energy in the range of natural frequencies of hull vibration.

The present investigation is entirely empirical, but it is set and motivated within the framework and understanding introduced above. Some interesting, stationary records of measured stresses are selected from the available data. The high frequency, vibratory component is filtered out, leaving the stress signal in the wave frequency range, referred to as the low-pass signal. Local maxima and minima are picked out from the total and low-pass signals. Distribution functions are fitted to the local maxima and minima and used to estimate extreme values. Extreme values with and without the vibratory component are compared. Further details of this study may be found in [4].

2. AVAILABLE DATA

Measured data from two iron ore carriers are considered here. Ship X trades on the North Atlantic, while ship Y trades on both the North and South Atlantic. Principal dimensions of the two ships are listed in Table 1. The draughts given for ballast and loaded conditions are typical values and not necessarily identical to the conditions applicable during the measurements.

Both ships are fitted with strain transducers, attached to deck plating, in line with a longitudinal bulkhead, slightly forward of amidships, on port and starboard sides of the centreline, about halfway between the centreline and the deck edge. The strain signals are sampled at 25Hz. This relatively high, sampling frequency is intended to capture both stationary and transient hull girder response in accurate detail.

The ships also carry Wavex wave radars. Ship speed over ground, course made good and position are

available from the vessels' global positioning systems (GPS). Wind speed and direction are also recorded. The accuracy and interpretation of the metocean and ship parameters is discussed in [1], [2] and [4]. The wave data is not very accurate for ship Y, possibly overestimating the wave height by 20% [2]. The wave height estimates from ship X were improved after its hull was strengthened, a few years ago, and the present data from this ship is considered to be more reliable than hindcast data. Additional wave data has been obtained from the ARGOS satellite and used in evaluation of the wave radar, but the satellite data only provides sparse coverage of the conditions that the vessels experience [4]. Further details of the instrumentation are given in [1] and [5].

	Ship X	Ship Y
Length between perpendiculars (m)	294	281
Beam, moulded (m)	53	48
Depth, moulded (m)	24.6	23.7
Scantling draught (m)	18.8	17.36
Scantling block coefficient	0.824	0.841
Ballast draught AP (m)	11.29	11.90
Ballast draught FP (m)	12.17	11.81
Loaded draught AP (m)	18.10	17.14
Loaded draught FP (m)	19.20	16.16

Table 1: Principal dimensions of the ships.

The present measurement systems have been in operation for about 5 years on ship X and for about 2 years on ship Y. A set of measurement data is initially accumulated on board for a number of voyages, and retrieved for further analysis ashore, at somewhat irregular intervals. The data storage system accumulates time series, each of length 30 minutes, from the 500 most severe strain conditions encountered during the voyages in each interval (of up to one year). Each 30-minute time series is further subdivided into 6 data blocks of 5 minutes. A computer program was written to reassemble a set of measured data into as long continuous time series as possible from the measured data. This is feasible, because several of the severe cases tend to arise from the same storm and are adjacent in time. A small number of these time series were selected for detailed analysis. The selection was intended to include the most severe strains that had been encountered, and to cover a range of conditions of varying intensity, but was not based on a systematic scan of all the intervals.

A detailed description of the analysis of a single, long time series follows in the next section. Results from all the selected time series are summarised in section 4.

3. ANALYSIS OF A TIME SERIES

This section describes the analysis of the strain time series labelled as X-B14 in Table 3; i.e. it refers to ship X

in the ballast condition. The measured strains are converted to stresses using Hooke's law; i.e. multiplied by Young's modulus. Stresses are intended to provide a better basis for an intuitive understanding of the severity of the measured hull response. A hogging condition leads to positive stress (maxima), while a sagging condition leads to negative stress (minima) in this system. Only the signal from the port transducer is considered. Some effect of horizontal bending of the hull girder is present in the signal, but this is expected to be small compared to the effect of vertical bending, as indicated by [5]. Axial load on the hull girder is naturally also present in the measured strain, but it is expected to be an order of magnitude lower than the bending stress, as indicated by [6].

3.1 STATIONARITY

It is essential that the time series can be regarded as stationary with respect to the analysis that is carried out here. This is also the prevalent assumption in the corresponding step in analytical models for ship response predictions. Stationarity implies that wave and ship conditions are constant in an appropriate statistical sense; i.e. significant wave height H_{mo} , peak wave period, ship heading relative to the waves, ship speed and cargo and ballast weights are constant. More strict conditions should ideally be imposed (e.g. concerning the wave spectrum), but the given set of parameters provides a practical compromise.

The original time series is not necessarily stationary. Hence, some means of establishing a stationary length of the time series is required. The present time series has a total duration of 29½hr. It is split into a sequence of sub-sections of 30min. duration each. Several statistics are calculated from each sub-section of the stress signal. The trends in these statistics are evaluated to identify a stationary portion. These statistics include the mean value, standard deviation, skewness, kurtosis and various spectral periods. Non-stationary mean values are considered acceptable. They are assumed to be primarily due to thermal stress, which varies with the sunlight, and does not affect the wave-induced response. This effect is filtered out, as described in section 3.3. The standard deviations of the stress signals, separated into low-pass and high-pass components, have provided the main indicator of stationarity, as illustrated in Figure 1. The triangular symbols on the figure show the computed standard deviations for each 30-minute segment, the continuous horizontal line shows the standard deviation computed for the entire duration, and the chain-dotted line shows the linear trend. Some scatter, or statistical uncertainty, must be expected, whether or not the stress process is stationary. A coefficient of variation of about 5% would be expected for standard deviations computed from 30-minute segments of a comparable stationary process. The sequence comprising segments 10 to 30, from 16200s to 54000s after the beginning of the time series, is judged to be stationary. Only this part of the signal is utilised in the subsequent analysis, and forms the basis for Figure 2 to Figure 14 .

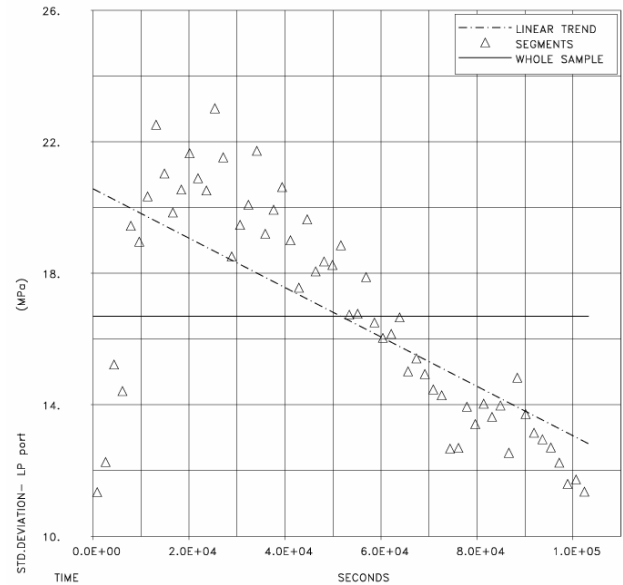


Figure 1 Stationarity check - standard deviations of low-pass stress from 30-minute sequences along a time series of 29.5hr, from case X-B14, starting at 0930hrs on 2005-01-11.

Further checks have been carried out against the measured significant wave height, the wave heading relative to the ship and the ship speed. The variations in these parameters were also found to be sufficiently small over the selected interval, so as to allow the assumption of stationarity to be maintained. The ship was making about 3½ knots in head seas with a significant wave height of 7.7m, according to the wave radar.

It was fortunate to find such a long, stationary, time series. This implies that statistical uncertainty is reduced as compared to results from shorter time series, which is particularly important when we attempt to draw conclusions concerning extreme stresses.

3.2 RESPONSE SPECTRUM

The power spectral density of the stress signal is shown in Figure 2. The vibratory stress component may be seen at 0.58Hz, which corresponds to the two-node mode of vertical hull bending in ballast condition. A little energy may be found at higher order modes, but this seems negligible in this linear graph. The low-pass signal, at about 0.08Hz or a period of 13s, is the dominant component, corresponding to the encounter frequency of the waves.

Finite impulse response filters are applied, in the time domain, to separate the low-pass and high-pass components, with cut-off frequencies of 0.4Hz. Variations in the mean value and any high frequency noise are also filtered out, with cut-off frequencies of 0.01Hz and 3.0Hz, respectively. The main effect of the filtering is illustrated in Figure 3 to Figure 6. The two pairs of figures show the stress signal in the vicinity of largest and 2nd largest stress events observed in this time series. Figure 3 shows the total signal and the low-pass

signal in the vicinity of the largest peak. The filtering process smoothes the signal and truncates the peaks and troughs. The mean stress, of about 38MPa, has also been eliminated. The corresponding high-pass signal is shown in Figure 4. Note the difference in scale between these two figures. The rapid increase in peak heights in Figure 4 may possibly indicate some form of impact excitation, but not from a single, short, impulsive loading. Note that the first significant vibration occurs during the hogging part of the cycle as seen in Figure 3. Hence it does not look like the usual form of whipping, as seen during the sagging part of the cycle, and arising from stem/bow flare impacts, while the bow is deeply submerged.

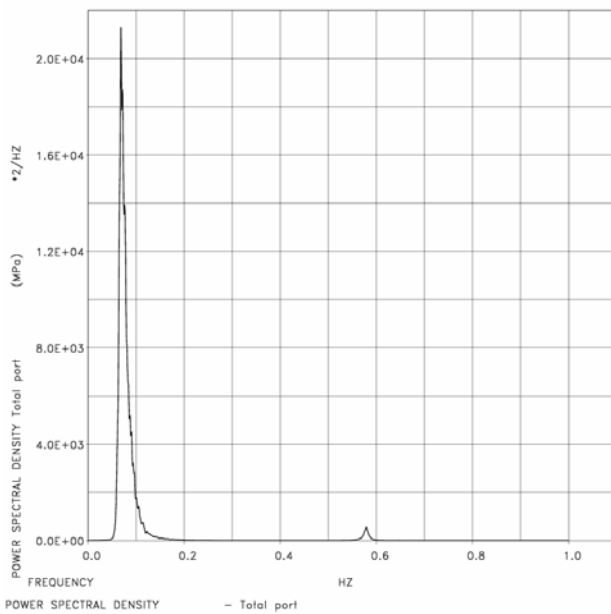


Figure 2 Power spectral density of stress signal.

3.3 FILTERING AND LARGEST PEAKS

Due to the large difference in periods between the wave frequency loading and the vibratory loading, the vibration tends to provide an increase in the maximum stress, similar to superposition. Note also that the section modulus for the measurement position in the deck is about 50% above the IACS requirement, hence about 50% higher measured stresses would be expected in a similar ship with optimized scantlings.

Figure 5 and Figure 6 provide a corresponding visualisation in the vicinity of the second largest peak stress event. In this case, the peak amplitude of the high-pass signal is only about half as large as in Figure 4. We apologise for the poor resolution of the labelling on the time axes in these figures.

There also seems to be an unusually large difference between the peak stresses in the largest event in Figure 3 and the 2nd largest in Figure 5. This large difference is the reason for the deviations in the tails of the fitted distributions in Figure 10 and Figure 12, below. We may wonder if a rare wave event has occurred, or if some

brief variation in heading or speed lies behind the largest event, but we lack data to investigate this.

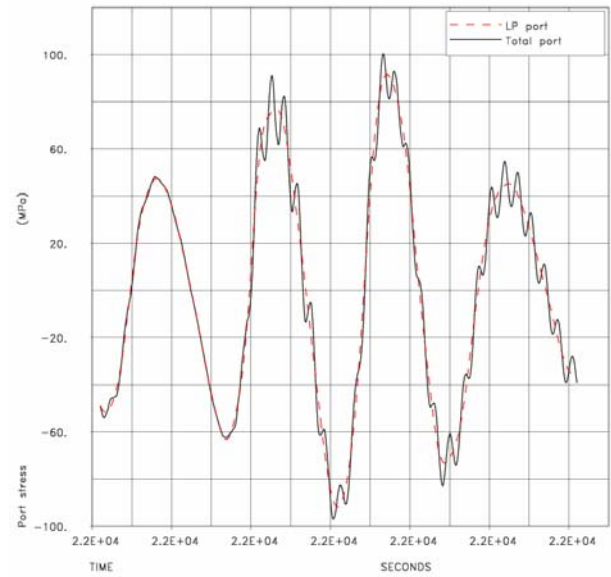


Figure 3 Total and low-pass stress signals in the vicinity of the largest observed maximum.

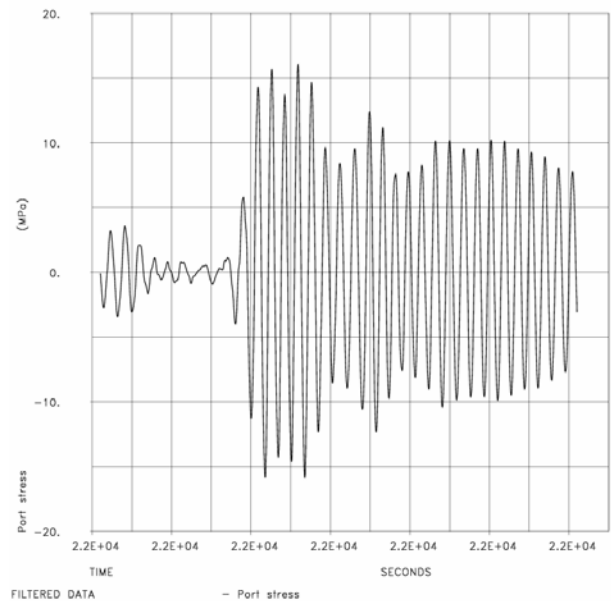


Figure 4 High-pass stress signal in the vicinity of the largest observed maximum of the total stress.

3.3 DISTRIBUTION OF CONTINUOUS SIGNAL

Empirical probability density functions are estimated from all the sampled points of the low-pass and high-pass signals, and shown in Figure 7 and Figure 8. Normal probability density functions are also fitted to these data sets and shown in the figures. The normal distribution appears to provide a good fit to the low-pass signal in Figure 7. This is usually expected in linear theory, from a Gaussian wave process and a linear ship response.

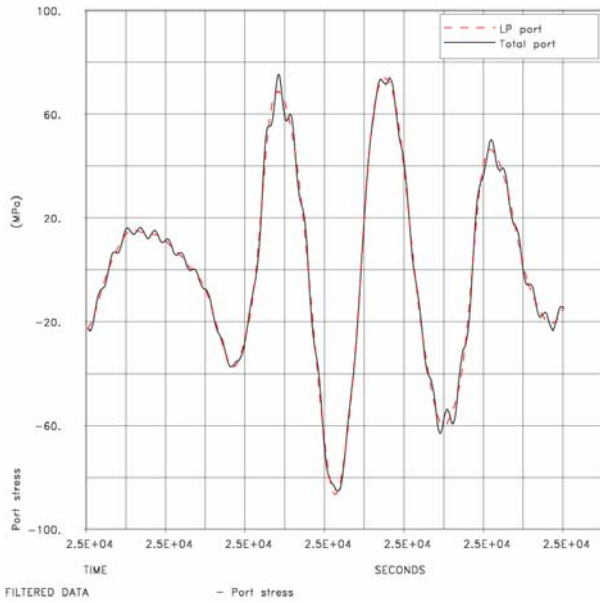


Figure 5 Total and low-pass stress signals in the vicinity of the 2nd largest observed stress event.

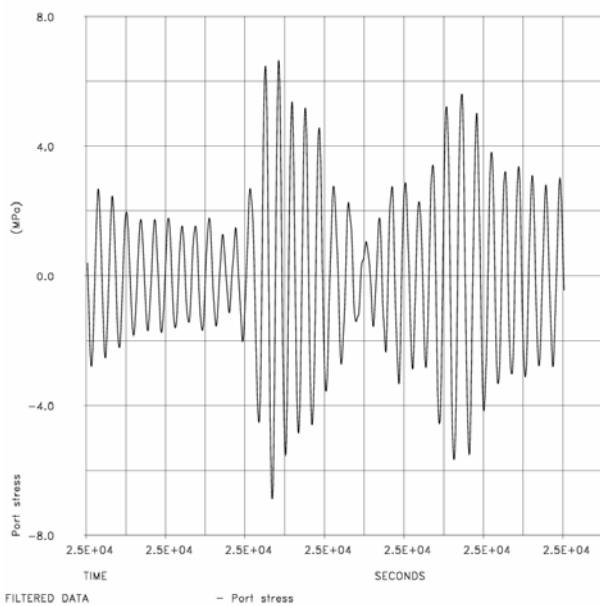


Figure 6 High-pass stress signal in the vicinity of the 2nd largest observed stress event.

On the other hand, the normal distribution does not appear to provide a good fit to the high-pass signal in Figure 8. More probability mass is located near the mean and in the tails of the empirical density. These results indicate that an assumption of a normal distribution would be inappropriate for the high-pass stress component. It may be tempting to speculate that vibration at high and low levels are caused by different mechanisms, such as springing and whipping, but there is no clear proof of this. Whipping response may occur only occasionally, giving some high vibration cycles, but many small cycles due to a slow decay with low damping, at about 0.5% of critical damping [3]. Springing response also normally gives many small

vibration cycles. This may explain the behaviour, which has not been observed in other literature; e.g. [5] and [7].

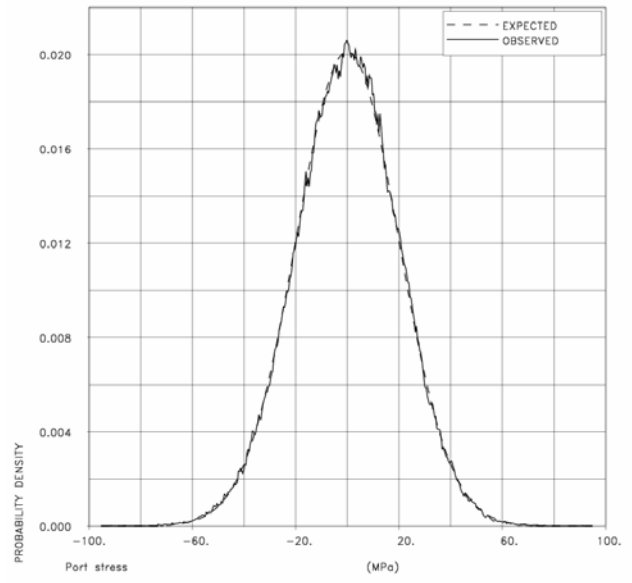


Figure 7 Empirical probability density function of the continuous, low-pass, stress signal together with a fitted normal density function.

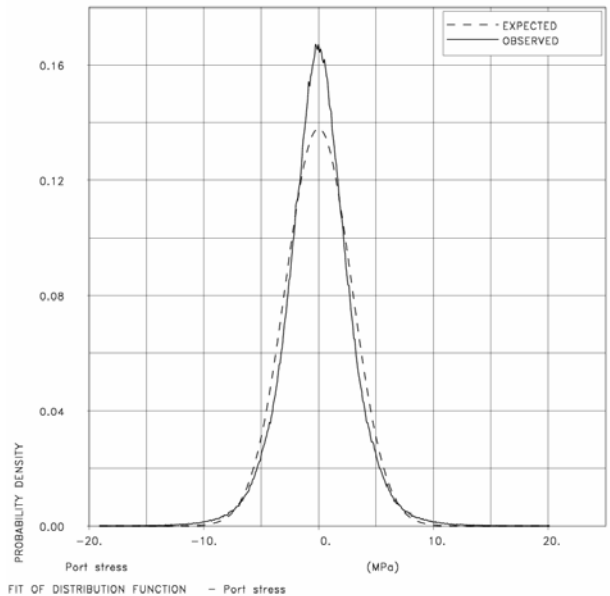


Figure 8 Empirical probability density function of the continuous, high-pass, stress signal together with a fitted normal density function.

3.5 DISTRIBUTION OF MAXIMA AND MINIMA

It is desirable to find a distribution function which adequately fits the response maxima and minima, for use in both the empirical prediction of extreme values and in theoretical analyses. There is some difficulty in selecting appropriate sets of local maxima and minima, for use in the fitting process, from the time history of the total and low-pass signals. The present approach concentrates on the higher peaks and lower troughs of the dominant, low-

pass stress signal and how they are affected by the vibratory stress, in the total signal. This implies that a large number of additional, local peaks and troughs due to the vibratory stress are excluded. The selection algorithm for maxima includes the following steps:

- All local maxima are initially identified and selected,
- Maxima less than a threshold level of 0.1 standard deviations above the mean level of the continuous signal are excluded,
- Maxima that are separated by less than a certain time window are excluded, such that the larger value is retained from each comparison. This time window is set at 70% of the mean period of the low-pass signal for each stationary time series.

Some sensitivity checks have been carried out on the values of the threshold (0.1, 0.2 & 0.5 std. dev.) and the time window (11s & 8s) parameters. The larger stress maxima are insensitive to the parameter values, while the total number of maxima is slightly affected by the threshold level, and more strongly affected by the time window. The present choice of parameters seems acceptable, since we are primarily interested in the distribution of the larger stress maxima. A corresponding selection algorithm is applied to the stress minima.

Weibull probability distributions are fitted to the selected sets of stress maxima and minima. Experience shows that this type of distribution often provides quite a good fit to slightly nonlinear, wave-induced response. The Weibull distribution of a random variable X may be written as

$$F_X(x) = 1 - \exp\left\{-\left(\frac{x-\gamma}{\alpha}\right)^\beta\right\}$$

where α is the scale parameter, β is the shape parameter and γ is the location parameter. The method of moments is applied in the fitting process. The Rayleigh distribution, which is widely applied to linear, wave-induced responses, forms a subset of the Weibull distribution, with shape parameter $\beta = 2$ and location parameter $\gamma = 0$.

The empirical probability density of maxima from the total stress is compared to the fitted density in Figure 9, while the corresponding distributions are compared in Figure 10. 2814 maxima are included in this data set. The fitted parameters are listed in Table 2. The figures indicate that a good fit is obtained.

Similar comparisons for the low-pass stress maxima are shown Figure 11 and Figure 12, with the fitted parameters in Table 2. There are 2782 maxima in this data set, somewhat less than in the total signal. Corresponding comparisons for the minima from the total signal and the minima from the low-pass signal are not shown here, but the fits are of comparable quality and

the fitted parameters are included in Table 2. Note that the fitted shape parameter is fairly close to the value for the Rayleigh distribution, $\beta = 2.0$, in all 4 cases. It is not clear if the deviations away from this value are significant.

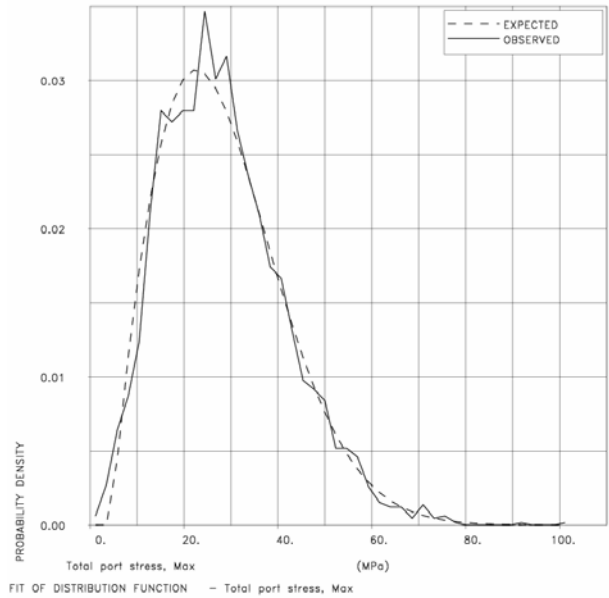


Figure 9 Empirical probability density function of the maxima, of the total stress signal together with a fitted Weibull density function.

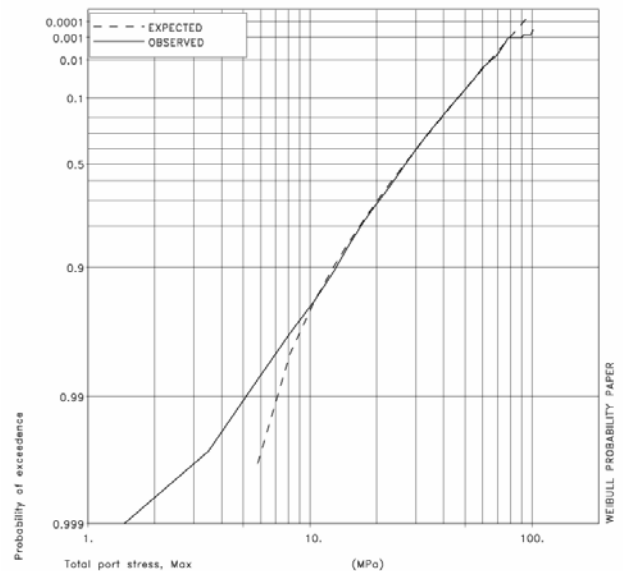


Figure 10 Empirical distribution function of the maxima, of the total stress signal together with a fitted Weibull distribution.

Case	Weibull parameters		
	α (MPa)	β	γ (MPa)
Total maxima	26.88	1.885	4.58
Low-pass maxima	24.88	1.886	3.68
Total minima	29.99	1.875	4.46
Low-pass minima	25.38	1.827	3.71

Table 2: Weibull distribution parameters fitted to maxima and minima of total and low-pass stress.

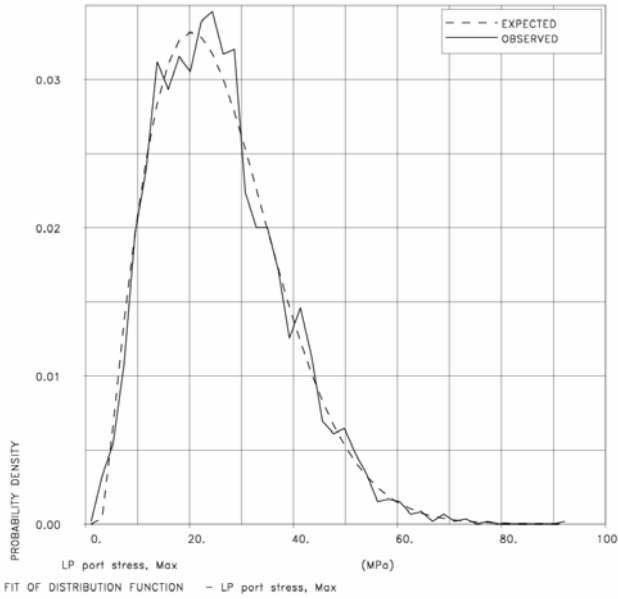


Figure 11 Empirical probability density function of the maxima, of the low-pass stress signal together with a fitted Weibull density function.

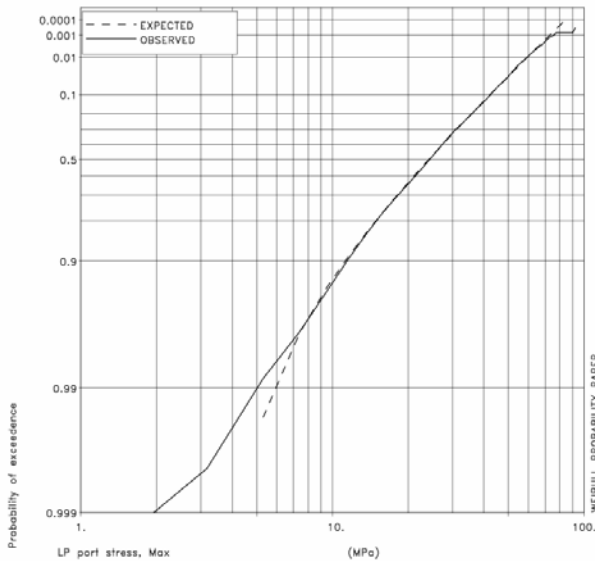


Figure 12 Empirical distribution function of the maxima, of the low-pass stress signal together with a fitted Weibull distribution.

The empirical distributions of stress maxima from the total and low-pass signals are compared in Figure 13. The increase in stress due to the hull girder vibrations is clearly shown by this figure. A similar comparison of the stress minima is shown in Figure 14. The difference in the numbers of extrema, between the total signal and the low-pass signal, with more small values from the total signal due to the high frequency component, is the reason why the curves cross each other.

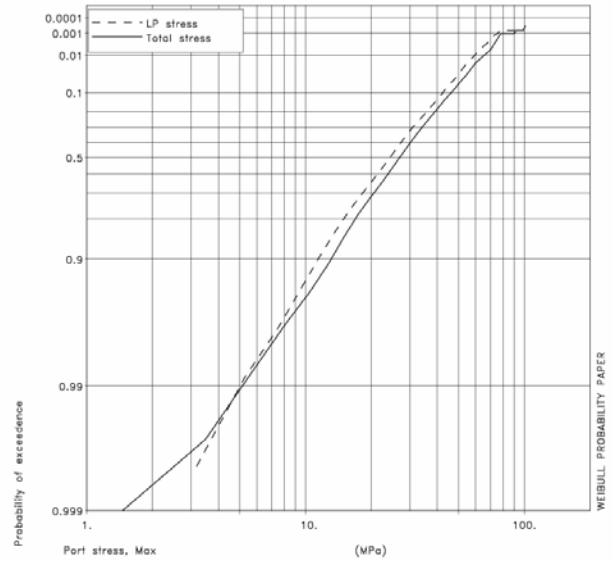


Figure 13 Comparison of empirical cumulative distributions of local stress maxima; from total signal and from low-pass signal.

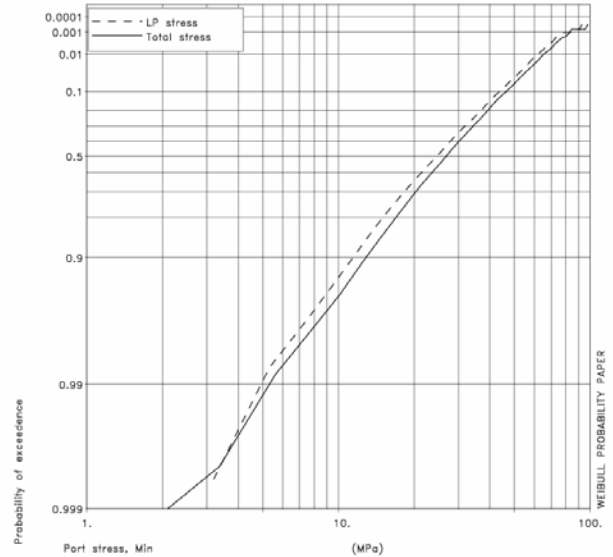


Figure 14 Comparison of empirical cumulative distributions of local stress minima; from total signal and from low-pass signal.

It is noted that the maximum in hogging is very similar to the maximum in sagging; i.e. the ratio between extreme sagging and hogging stresses must be close to 1.0 in this

sea state, and that is what we would expect for a ship with vertical sides in the vicinity of the water line.

4. TRENDS WITH CHANGING CONDITIONS

Wave and ship parameters from the selected cases are listed in Table 3 and Table 4, at the end of the paper. The corresponding results for the largest measured stress maxima and minima are listed in the same tables. Extreme values have also been estimated from the fitted distributions and show fairly similar trends, but are not included here.

The largest stresses are obtained from ship X in ballast condition, case X-B14. This is a case with very severe waves (H_{mo} of 7.7m from the Wavex and 9.5 to 12m from the Argoss), very low forward speed and near head seas, according to the somewhat uncertain parameters. The vibratory stress component contributes 9% to the hogging stress and 6% to the sagging stress. The total hogging stress exceeds the total sagging stress, while the low-pass filtered stresses are nearly equal in the opposed directions.

The largest relative contribution from the vibratory stress is obtained in case X-B11, with 51% added to the low-pass hogging stress and 33% to the low-pass sagging stress. This occurs in head seas, in moderately severe waves and with a moderate forward speed.

The results in the tables have been organised to facilitate inspection for some general trends. Results in ballast conditions are shown first, followed by loaded conditions. The draughts and weight distributions in these two conditions tend to be very consistent between voyages. Analysis of the mean periods of the high frequency stresses show:

- 1.74s for ship X in ballast,
1.61s for ship Y in ballast,
- 1.95s for ship X when loaded,
1.81s for ship Y when loaded.

These periods vary by little more than ± 0.02 s, and actually serve to provide a confirmation of the loading condition (note that the natural frequencies are about 10% higher for these two ships compared to ships with conventional strength [1], [2]). The relative vibratory contributions to the peak stresses appear to be somewhat higher in ballast than in corresponding loaded conditions, though the number of loaded cases is rather small for a convincing comparison. This tendency coincides with our expectations concerning excitation forces; viz. more possibilities for bottom impact at ballast draught and less attenuated 2nd order pressures on the ship bottom.

The results are sorted by heading category within each loading condition, with the expectation that some trends can be identified in head and aft seas, while behaviour in beam seas is likely to be more difficult to interpret

without accurate measurement of wave spectra. The mean periods of the low-pass stresses show fairly clear differences with heading category:

- from 9.7 to 12.8s in head seas
- from 16.7 to 18.9s in aft seas.

The relative contribution of the vibratory component tends to be quite small in aft seas. This interpretation is somewhat uncertain due to the limited amount data suitable for comparison.

Finally, the results are sorted by significant wave height within each heading category. There are a fair number of cases from ship X for ballast conditions in head seas. A tendency for reduced speed with increasing wave height is quite clear from these results. There also seems to be some tendency for a reduced relative contribution from the vibratory component with increasing wave height. However, the relative magnitude of the vibratory component varies rather irregularly, so more results are needed to confirm this.

Note also that the maximum hogging stress is often larger than the corresponding maximum sagging stress for the low-pass response. This is also interesting, and not reflected in the literature.

5. CONCLUSIONS

A pilot study has been carried out to investigate if wave-induced hull girder vibrations contribute significantly to extreme stresses in bulk carriers. Long term, full scale measurements, primarily designed to investigate fatigue, have been utilised for this purpose. Stress extrema, with and without the vibratory component, have been compared on the basis of measurements from stationary conditions. Relatively long time series have been used in order to reduce statistical uncertainty. The increase due to the vibratory component ranges from nothing up to 50%. In the most severe waves that were encountered, the increases were 10% in the hogging stress and 5% in the sagging stress. This indicates that the vibratory response may possibly contribute significantly to the ultimate limit state for bulk carriers. It should be noted that really extreme sea states (e.g. around 15m significant wave height) have not been encountered during this measurement programme and that there is significant uncertainty about the relative contribution of vibratory response in such sea states, since a significant part of the ship's bottom may actually come out of the water.

It is recommended to extend this study to a larger set of cases.

6. ACKNOWLEDGEMENTS

We would like to thank the owners of the vessels for the use of the measurement data and to acknowledge the contributions of many colleagues in these measurement programmes. The opinions expressed in the paper by the authors do not necessarily represent the views of the Det Norske Veritas.

7. REFERENCES

- [1] Moe, E., Holtsmark, G., Storhaug, G., 'Full scale measurements of the wave induced hull girder vibrations of an ore carrier trading in the North Atlantic,' RINA, Int. Conf. Design & Operation of Bulk Carriers, London, 2005.
- [2] Storhaug, G., Moe, E. and Holtsmark, G., 'Measurements of wave induced hull girder vibrations of an ore carrier in different trades', Proceedings of OMAE, 2006.
- [3] Slocum, S., 'Theoretical evaluation of nonlinear springing excitation and response', PhD dissertation, University of Michigan, 1983
- [4] Kjelstadli, R.Ø., 'Extrapolation of numerical analysis and full scale measurements to estimate the extreme loading of container vessels and bulk carriers,' Master thesis in Marine Technology, Norw. Univ. of Sci. & Techn., Trondheim, 2007.
- [5] Storhaug, G., Vidic-Perunovic, J., Rüdinger, F., Holtsmark, G., Helmers, J.B. and Gu, X., 'Springing/Whipping response of a large ocean going vessel – a comparison between numerical simulations and full scale measurements', Proc. 3rd Int. Conf. on Hydroelasticity in Marine Technology, Oxford, 2003.
- [6] Storhaug, G. and Moe, E., 'Measurements of wave induced vibrations onboard a large container vessel operating in harsh environment', Proc. PRADS, 2007.
- [7] Gran, S., 'Statistical description of wave induced vibratory stresses in ships', DNV report no. 80-1171, 1980.

8. AUTHORS BIOGRAPHY

Jan Mathisen holds the current position of a Principal Engineer with DNV Energy in the section for risers, moorings and umbilicals. He has often dealt with the analysis of time series, since joining DNV in 1971 and during research for a PhD from Brunel University in 1988. Email: Jan.Mathisen@dnv.com.

Robert Kjelstadli has recently joined DNV Maritime, in the section for tankers, after completing his Master of

Technology degree, in Naval Architecture & Ocean Engineering, at the Norwegian University of Science & Technology. Email: Robert.Ostraat.Kjelstadli@dnv.com

Gaute Storhaug holds the current position of Senior Engineer in the section for hydrodynamics, structures and stability in DNV. He is responsible for full scale measurements, as well as fatigue calculations, within the condition assessment programme for old tankers. His previous experience includes full scale measurements, model experiments and hydrodynamic and structural analysis of container vessels and bulk carriers, as well as tankers, shuttle tankers and LNG vessels related to the additional class notation HMON. Some of the projects and vessels have also been part of trouble shooting services and DNV research including PhD research at the Centre of Excellence for Ships and Ocean Structures at the Norwegian University of Science and Technology, NTNU. Email: Gaute.Storhaug@dnv.com

Erlend Moe is employed as ship surveyor at DNV, Bulk Carriers and Container Ships. He graduated with a M.Sc. in marine structures from the NTNU in 1999. Email: Erlend.Moe@dnv.com

Key to abbreviations in Table 3 & Table 4, below:

Case ID: 1st letter indicates the ship (X or Y), 2nd letter indicates ballast (B) or loaded (L), and the number is just a sequence number.

Relative wave direction 0° represents head seas, 90° is for beam seas from the starboard side and 180° is for following seas. Heading category A is for aft seas (180°±30°), H is for head seas (0°±30°) and B is for beam seas (from 30° to 150° and from 210° to 330°).

Results are ordered by: (1) loading condition, (2) heading category, (3) by significant wave height.

The largest total stress and low-pass filtered stress is given for each case, relative to the mean level during the case. The percentage increase of the total stress relative to the low-pass stress is also included.

Case ID	Date	Rel. hdg. (deg.)	Heading. cat.	Wave H_{m0} (m)	Ship speed (m/s)	LP period (s)	Duration (hrs)	Hogging stress			Sagging stress		
								Total (MPa)	LP (MPa)	Incr. %	Total (MPa)	LP (MPa)	Incr. %
X-B1	2006-01-05	31	B	4.7	5.1	9.5	3.0	50.7	38.6	31%	39.4	28.6	38%
X-B2	2004-11-20	139	B	5.9	7.2	16.3	3.5	58.7	58.9	0%	50.0	47.9	4%
X-B3	2005-12-11	225	B	6.2	6.2	16.0	3.5	43.7	42.5	3%	40.8	40.2	1%
X-B4	2005-03-12	135	B	6.9	6.5	16.0	2.5	67.6	65.5	3%	62.7	59.3	6%
X-B5	2004-11-19	294	B	7.0	4.0	11.2	3.0	56.7	50.0	13%	45.0	40.6	11%
X-B6	2006-01-05	0	H	4.0	5.5	10.7	3.0	40.8	35.4	15%	43.2	34.1	27%
X-B7	2005-12-08	357	H	4.7	5.0	10.8	3.0	48.4	40.8	19%	44.0	35.2	25%
X-B8	2005-01-10	333	H	4.9	4.6	10.5	4.0	53.3	45.0	18%	48.4	45.6	6%
X-B9	2005-12-08	349	H	4.9	4.6	11.7	4.0	70.7	66.1	7%	58.1	56.9	2%
X-B10	2005-02-09	28	H	5.0	5.0	10.7	1.5	45.3	39.3	15%	40.3	31.0	30%
X-B11	2006-01-07	5	H	5.3	4.2	10.4	3.0	57.6	38.2	51%	50.2	37.8	33%
X-B12	2004-12-16	340	H	5.4	3.6	9.9	3.0	59.6	45.1	32%	53.5	40.3	33%
X-B13	2005-01-13	3	H	6.9	3.8	12.4	2.5	73.4	66.2	11%	73.3	72.1	2%
X-B14	2005-01-11	358	H	7.7	1.8	12.8	10.5	100.0	91.4	9%	97.0	91.9	6%
X-L15	2004-12-28	209	A	4.6	7.0	16.8	5.0	43.8	43.4	1%	46.7	46.1	1%
X-L16	2004-11-28	179	A	5.2	7.0	18.9	2.0	41.3	41.1	0%	41.6	41.5	0%
X-L17	2004-11-29	200	A	6.0	7.0	18.4	3.5	48.8	47.7	2%	49.1	49.0	0%
X-L18	2005-01-26	58	B	5.2	4.7	11.1	2.5	53.8	51.0	5%	46.0	46.3	-1%
X-L19	2006-03-09	216	B	5.3	6.7	16.3	3.0	40.5	40.7	0%	39.9	40.3	-1%
X-L20	2005-01-24	23	H	6.6	2.0	11.0	3.5	65.4	64.9	1%	63.0	55.1	14%

Table 3: Results from ship X. (Please confer key above Table 3.)

Case ID	Date	Rel. hdg. (deg.)	Head-ing. cat.	Wave H_{m0} (m)	Ship speed (m/s)	LP period (s)	Dura-tion (hrs)	Hogging stress			Sagging stress		
								Total (MPa)	LP (MPa)	Incr. %	Total (MPa)	LP (MPa)	Incr. %
Y-B1	2005-03-17	182	A	5.7	8.1	16.7	0.5	30.1	30.1	0 %	26.8	26.2	2 %
Y-B2	2005-03-18	160	A	8.0	7.3	17.3	1.5	43.3	37.2	16 %	39.6	37.0	7 %
Y-B3	2005-04-12	95	B	5.7	5.4	8.6	0.5	39.0	33.0	18 %	31.4	25.2	25 %
Y-B4	2005-04-06	68	B	5.9	4.5	8.9	0.5	49.7	34.5	44 %	33.3	22.2	50 %
Y-B5	2005-03-15	32	B	7.0	2.7	11.4	3.0	66.8	51.4	30 %	70.8	57.4	23 %
Y-B6	2005-03-14	345	H	4.8	6.0	9.7	1.5	47.8	40.4	18 %	42.7	36.8	16 %
Y-L7	2005-06-03	111	B	0.6	---	15.8	0.5	6.3	6.3	0 %	8.1	8.1	1 %
Y-L8	2005-06-03	251	B	4.3	---	16.4	3.5	14.8	14.5	2 %	13.0	12.9	1 %
Y-L9	2005-05-29	274	B	4.4	---	14.0	3.0	19.0	17.6	8 %	21.3	20.5	4 %
Y-L10	2005-03-04	94	B	6.9	4.5	10.8	3.5	60.7	47.7	27 %	50.2	39.2	28 %
Y-L11	2005-03-05	128	B	7.1	5.6	11.3	0.5	35.9	31.4	14 %	33.2	30.0	11 %

Table 4: Results from ship Y. (Please confer key above Table 3.)